Geophysical Research Letters

RESEARCH LETTER
10.1029/2020GL087477

Key Points:
- We examine the scaling properties of slow-slip events using dynamic simulations of frictional sliding
- Our results match observations from the Cascadia subduction zone, including the earthquake-like cubic moment-duration scaling
- Slow-slip events are consistent with ordinary earthquake scaling due to magnitude-dependent rupture speed and stress drop

Supporting Information:
- Supporting Information S1

Correspondence to:
L. Dal Zilio,
dalzilio@caltech.edu

Citation:
Dal Zilio, L., Lapusta, N., & Avouac, J.-P. (2020). Unraveling scaling properties of slow-slip events. *Geophysical Research Letters*, *47*, e2020GL087477. https://doi.org/10.1029/2020GL087477

Received 11 FEB 2020
Accepted 9 MAY 2020
Accepted article online 12 MAY 2020

Author Contributions
Conceptualization: Luca Dal Zilio, Nadia Lapusta, Jean-Philippe Avouac
Methodology: Luca Dal Zilio, Nadia Lapusta, Jean-Philippe Avouac
Writing - Original Draft: Luca Dal Zilio, Nadia Lapusta, Jean-Philippe Avouac
Formal Analysis: Luca Dal Zilio, Nadia Lapusta, Jean-Philippe Avouac

Unraveling Scaling Properties of Slow-Slip Events

Luca Dal Zilio[1,2], Nadia Lapusta[1,2], and Jean-Philippe Avouac[1,2]

[1]Division of Geological and Planetary Sciences, California Institute of Technology, Pasadena, CA, USA, [2]Division of Engineering and Applied Sciences, California Institute of Technology, Pasadena, CA, USA

Abstract A major debate in geophysics is whether earthquakes and slow-slip events (SSEs) arise from similar failure mechanisms. Recent observations from different subduction zones suggest that SSEs follow the same moment-duration scaling as earthquakes, unlike qualitatively different scaling proposed by earlier studies. Here, we examine the scaling properties using dynamic simulations of frictional sliding. The resulting sequences of SSEs match observations from the Cascadia subduction zone, including the earthquake-like cubic moment-duration scaling. In contrast to conventional and widely used assumptions of magnitude-invariant rupture velocities and stress drops, both simulated and natural SSEs have rupture velocities and stress drops that increase with event magnitudes. These findings support the same frictional origin for both earthquakes and SSEs while suggesting a new explanation for the observed SSEs scaling.

Plain Language Summary Tectonic faults produce a wide spectrum of slip modes, ranging from fast earthquakes to slow-slip events. Whether slow-slip events and regular earthquakes result from a similar physics is debated. Here we present numerical simulations to show that slow-slip events can result from frictional sliding like seismic slip, with an additional mechanism that prevents acceleration to fast slip due to the presence of fluids. The model succeeds in reproducing a realistic sequence of slow-slip events and provides an excellent match to the observations from the Cascadia subduction zone, including the observation that the moment, which quantifies the energy released by fault slip, is proportional to the cube of the duration. Importantly, our study demonstrates that this scaling arises for different reasons from the traditional explanation proposed for regular earthquakes.

1. Introduction

The discovery of slow-slip events (SSEs) has revolutionized our understanding of how tectonic faults accommodate long-term slip motions (Bürgmann, 2018; Dragert et al., 2001; Ozawa et al., 2002). Faults were previously thought to release stress either through steady aseismic sliding, or through earthquakes resulting from abrupt failure of locked faults. In contrast, SSEs appear to spontaneously accelerate but proceed much slower than traditional earthquake ruptures (Obara et al., 2004; Rogers & Dragert, 2003). On the Cascadia megathrust (Michel et al., 2018), as in many circum-Pacific subduction zones (Schwartz & Rokosky, 2007), SSEs slide at rates between 10 and 100 times higher than the plate convergence rate for a few days to a few weeks, accumulating centimeters of slip (Figure 1a). They occur in a narrow yet long section of the plate interface deeper than the locked zone, which often coincides with the intersection of the fore-arc Moho and the subduction interface (Figure 1b) (Gao & Wang, 2017). The most recent catalog of SSEs from this region was obtained from the inversion of geodetic position time series recorded at 352 continuous GPS stations between 2007 and 2017 (Michel et al., 2018). The catalog of SSEs extracted from the inferred slip history on the whole megathrust contains 64 events, which were found to coincide with the spatiotemporal distribution of tremors. The analysis of this catalog revealed that the SSEs occurred as unilateral or bilateral pulse-like ruptures with average rupture speed between ~5.5 and ~11 km/day.

A fundamental characteristic—viewed as a window into physical mechanisms of slow and fast rupture—is the relation between event moments (M; defined as the integral of slip over the rupture area multiplied by the shear modulus) and their duration (T). Regular fast earthquakes have long been known to follow a cubic moment-duration scaling relation for a wide range of event magnitudes ($M \propto T^3$) (Kanamori & Anderson, 1975). The cubic scaling is expected from the traditional representation of earthquake source as a circular rupture with spatially constant, magnitude-invariant stress drop expanding at a spatially constant, magnitude-invariant rupture speed—often simply called "a circular crack model" (Kostrov, 1964;

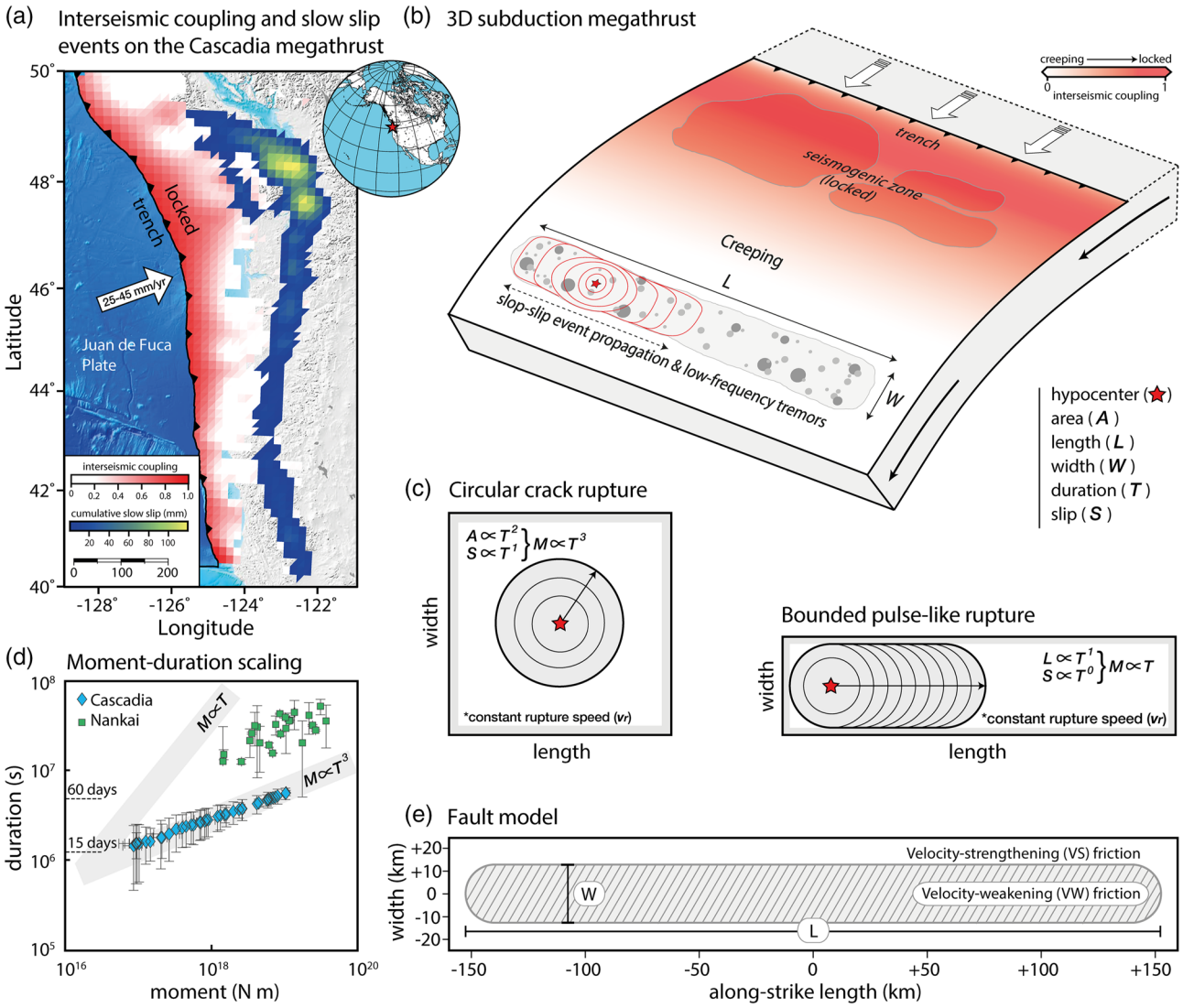

Figure 1. Interseismic coupling and SSEs in Cascadia, model setup, and traditional models for rupture scaling. (a) Comparison of interseismic coupling with cumulative slip due to episodic slow slip between 2007 and 2017 (Michel et al., 2018) showing that SSEs occur within the deeper creeping portion of the megathrust. The inset locates the main map. (b) Schematics of the source distribution for SSEs and deep low-frequency tremors at the downdip, interseismically creeping portion of the megathrust in Cascadia. (c) Conventional circular crack model, width-bounded pulse-like rupture model, and the associated scalings of different quantities with recurrence time. (d) Earthquake-like cubic moment-duration scaling observed in Cascadia (Michel et al., 2019) and Nankai (Takagi et al., 2019). (e) Our idealized model representation of the slow-slip-event region in Cascadia, with a velocity-weakening (VW; gray hashed region) strip within the otherwise velocity-strengthening region (VS; white) region of a rate-and-state fault.

Madariaga, 1976) (Figure 1c). The moment-duration scaling should switch to $M \propto T$ when slip events saturate the width (W) of the seismogenic zone (Figure 1c), thus propagating for much longer length (L) (Romanowicz & Rundle, 1993). A global compilation of SSEs was used to suggest that SSEs do follow such a linear moment-duration scaling (Ide et al., 2007). A possible explanation was that most of the detected SSEs have elongated rupture area, suggesting that—like large earthquakes—they might be geometrically bounded (Gomberg et al., 2016). However, the analysis of the 10-year-long data set of SSEs from Cascadia (Michel et al., 2019) leads to the cubic moment-duration scaling law similar to most earthquakes (Figure 1d). This finding is consistent with a recent catalog from the Nankai subduction zone (Takagi et al., 2019) and a study of SSEs using tremors in Mexico (Frank & Brodsky, 2019). These findings are surprising as the SSEs in this catalog are pulse-like ruptures with elongated slipping areas. They clearly do not conform to the circular crack model. In addition, despite the relatively short observational time span, the SSEs in Cascadia seem to follow the Gutenberg-Richter distribution of sizes (Michel et al., 2019; Wech et al., 2010).

In this study, we seek to understand how the recently discovered cubic moment-duration scaling properties of SSEs in Cascadia can be explained based on numerical simulations of spontaneous fault slip. Episodic SSEs have been generated in models with rate-and-state friction, a well-established empirical constitutive law for low-velocity fault strength capable of modeling a range of earthquake source phenomena (Dieterich, 2007) (see supporting information). On rate-and-state fault segments with velocity-weakening friction, SSEs occur when the slipping region is large enough to cause slip acceleration, as during earthquake nucleation, but too small for that slip event to reach seismic slip rates (Liu & Rice, 2005). Several variants of rate-and-state fault models can significantly extend the range of parameters suitable for SSEs, including changes from velocity-weakening to velocity-strengthening friction with increasing slip rates (Leeman et al., 2016; Shibazaki & Shimamoto, 2007), geometric complexities and roughness (Li & Liu, 2016; Ozawa et al., 2019; Romanet et al., 2018), and decreases in pore fluid pressure due to shear-induced dilatancy (Marone et al., 1990; Segall & Rice, 1995; Segall et al., 2010). SSEs can also be obtained in models of rate-and-state faults with velocity-strengthening friction and additional destabilizing effects, for example, poroelastic (Heimisson et al., 2019), and in models with viscoplastic bulk effects (Tong & Lavier, 2018). Here, we show that a model of SSEs on a rate-and-state fault with a depth-bounded velocity-weakening region (Figure 1e) can explain the cubic moment-duration scaling of slow slip observed in Cascadia. This is in contrast to conceptual assumptions of prior studies that such model geometry should result in linear moment-duration scaling.

2. Methods

We take advantage of the recently developed numerical methods (Lapusta & Liu, 2009; Noda & Lapusta, 2010), which allow us to resolve, in one model, long-term tectonic loading, steady fault slip, nucleation and propagation of SSEs, afterslip transients, and any regular seismic earthquake ruptures if they result. The model aims to mimic the Cascadia subduction zone: We consider a thrust fault segment embedded into an elastic medium, loaded by a downdip slip at the long-term slip rate (40 mm/year) and governed by rate-and-state friction and dilatancy effects (Figure 1e). The area with steady-state rate-weakening friction (VW), where SSEs can occur, is embedded in a rate-strengthening domain (VS). We describe the model ingredients and determination of SSEs in the supporting information (Tables S1 and S2). Our exploration of a range of rate-and-state parameters shows that SSEs appear in a parameter regime between steady slow slip and regular (fast) earthquakes (Figure S1), consistent with prior studies (Liu & Rice, 2005). We obtain the best fit to the observations in a model that includes dilatancy and the associated fluctuations in pore fluid pressure (Segall & Rice, 1995; Segall et al., 2010), which we present next. An extended description of the numerical technique, model setup, and modeling procedure is given in the supporting information.

3. Modeling Results

Our reference model results in a rich history of SSEs with spontaneous nucleation, slow ruptures, magnitudes ranging from M 5.3 to 6.7, and a wide spectrum of aspect ratios (Figure S2). A minimum magnitude of ~5.3 is obtained because, in our models, the nucleation size for the initiation of seismic, earthquake slip is larger than the width (W) of the velocity-weakening region (see supporting information). This means that, when a SSE initiates, it expands up to the width of the velocity-weakening region, with an approximate minimum area of $\sim W^2$. The resulting synthetic catalog of 76 events approximately obeys the Gutenberg-Richter relationship with a b value of ~1 (Figure 2a). The simulated sequences of SSEs include interevent loading, nucleation, growth, along-strike propagation, and arrest (Figure 2b). During the interevent period, creep penetrates into the rate-weakening patch, building conditions for slow-slip nucleation and thus causing the fault to creep at a rate similar to the long-term slip rate. When a SSE nucleates, it grows and expands in a semicircular fashion until it saturates the width of the rate-weakening patch and slows down in the vicinity of the velocity-strengthening region. The slip area is thus bounded updip and downdip by the transitions to the rate-strengthening domain, and rupture proceeds by propagating along strike. The event shown in Figure 2b propagates for more than 160 km along strike, and eventually arrests in the area of relatively unfavorable prestress (Figure S3). Slip rate evolution with time along the mid-depth of the velocity-weakening patch (Figure 2c) provides another illustration of how the event propagates through the fault. Notably, the rupture velocity is not constant: After the nucleation phase, the rupture front accelerates from ~7.6 up to ~9.7 km/day by exploiting a fault area with a relatively higher prestress. It then slows down to ~3.1 km/day and eventually arrests in the vicinity of the locked (and lower-stressed) patch. As a result, the slipping area

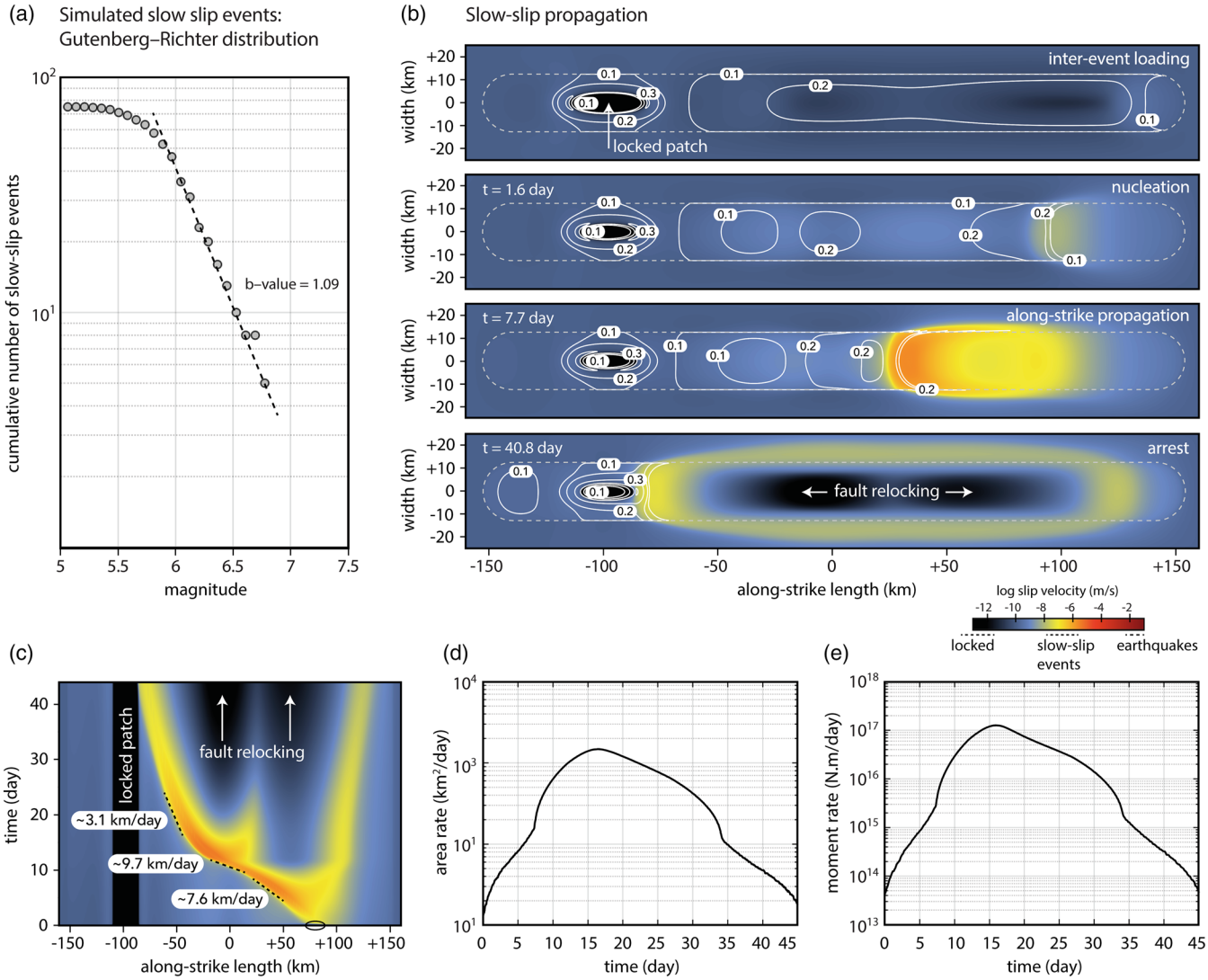

Figure 2. Simulated slow-slip events. (a) Gutenberg-Richter distribution of the simulated slow-slip event sequences. (b) Different stages in the long-term fault behavior given by snapshots of fault slip rates on a logarithmic scale, illustrating the time period around one slow-slip event. White contour lines define the regions with a prestress higher than average (in MPa). (c) Space-time evolution of the same event along the mid-depth of the velocity-weakening strip. (d and e) Temporal evolution of the slipping area and moment rate for the same event.

grows in the first half of the event and eventually shrinks before the end (Figure 2d). This variability, in turn, affects the source-time function (Figure 2e), which follows a near-triangular shape, despite the event appearing pulse-like due to its limited width.

We investigate the scaling properties of the simulated SSE population using the resulting synthetic data set, taking into account the sensitivity of the thresholds used to identify the duration, magnitude, and related uncertainties of each SSE (see supporting information and Figure S4). We find that the moments released by SSEs follow a cubic moment-duration scaling law ($M \propto T^3$; Figure 3a). This result emerges due to a combined effect of three different scaling properties. First, when the slipping area changes from that of expanding crack to pulse like and depth bounded, the rupture width remains constant in time ($W \propto T^0$). Second, the rupture length scales with the square of the event duration ($L \propto T^2$; Figure 3b). Third, the average slip scales linearly with the event duration ($S \propto T$; Figure 3c). Another emerging feature from our analysis is the moment-rupture area scaling, which results in the same $M \propto A^{3/2}$ scaling as for SSEs in Cascadia (Michel et al., 2019) and regular earthquakes (Kanamori & Anderson, 1975) (Figure 3d). Note that our modeling shows somewhat larger slip per duration and smaller rupture area per moment than the SSEs observed in Cascadia, yielding trend lines that are offset compared to the data from Cascadia but with very similar

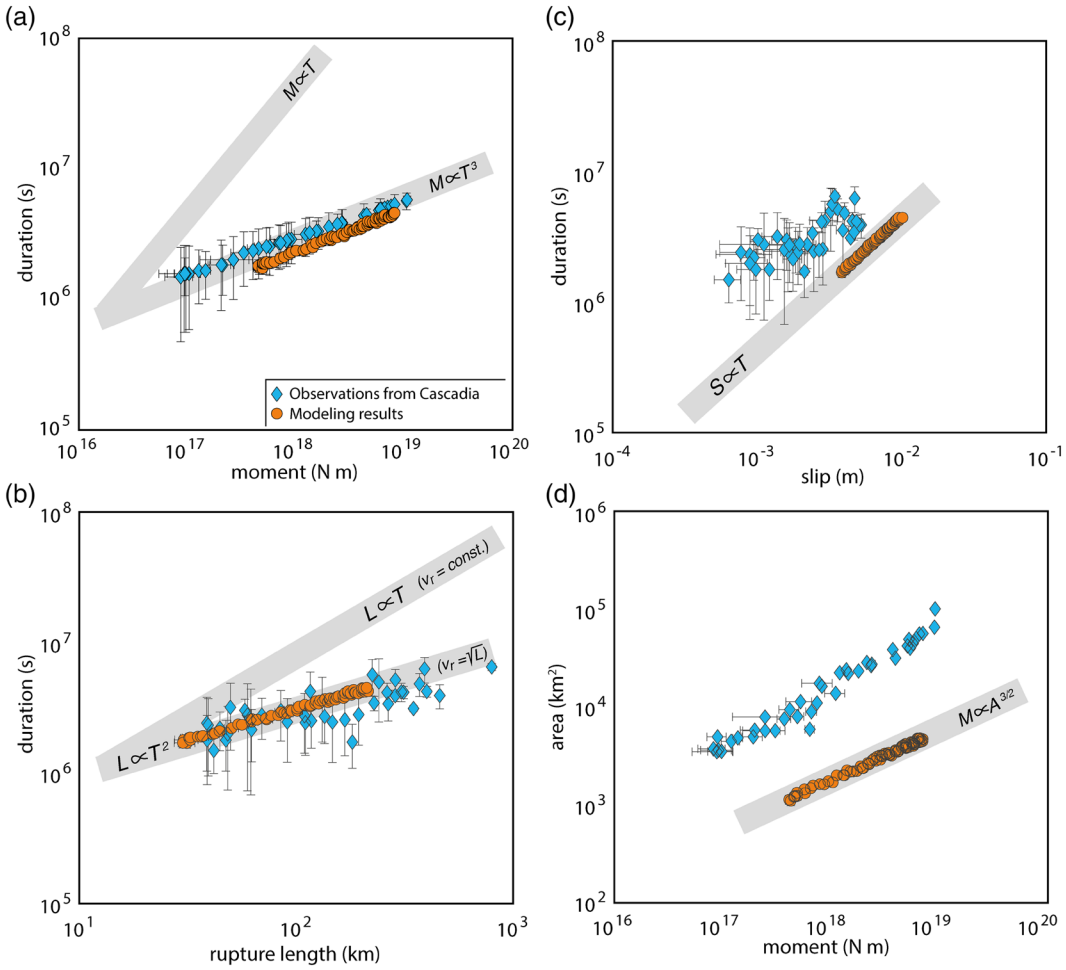

Figure 3. Comparison of scaling properties between the numerical experiments and observations from the Cascadia subduction zone. (a) Moment-duration scaling of SSEs in Cascadia (blue diamonds) (Michel et al., 2019) and simulated SSEs (orange dots). Gray shading illustrates the scaling trend of $M \propto T$ proposed for SSEs (Ide et al., 2007) and the earthquake-like scaling $M \propto T^3$ discovered for SSEs in Cascadia. (b) Rupture length L versus duration T, with both observations from Cascadia and simulated SSEs resulting in $L \propto T^2$, implying magnitude-dependent rupture velocity ($v_r = \sqrt{L}$). (c) Linear slip duration scaling, $S \propto T$. (d) Moment-rupture area scaling, $M \propto A^{3/2}$.

scaling. Part of this offset is because the width of SSEs in Cascadia is larger (~50 km) (Bartlow, 2020; Michel et al., 2019) and varies along strike, whereas our model adopts a fixed and smaller (25 km) width. However, natural SSEs clearly occur along a narrow and long band of the fault within the creeping region (Figure 1a). This means that SSEs increase in size primarily because of their increasing length. Also, the observational results may have higher rupture areas—and hence lower average slip per event—due to smoothing inherent in slip inversions, and that is why we did not seek a better fit. Although more computationally expensive, models with larger fault width W (and friction parameters with proportionally larger nucleation sizes and smaller stress drops) would provide an even better fit to observations.

Next, we examine the average rupture velocity (v_r) and stress drop ($\Delta\tau$) of each SSE, which are usually assumed and/or inferred to be magnitude-independent for regular earthquakes (Ide et al., 2007; Kostrov, 1964; Madariaga, 1976). Surprisingly, both Cascadia observations and our simulated SSEs show that rupture velocity increases with the event moment (Figure 4a) and follows the $M \propto v_r^3$ and $v_r \propto \sqrt{L}$ scalings (Figure S5). Similarly, we find that the average stress drop—calculated using the energy-based average measure (Noda et al., 2013)—increases with the moment of the event (Figure 4b). These results shed light on the dynamics of SSEs and explain the underlying mechanism for the observed scaling properties. In particular, they uncover new features of SSE dynamics: these pulse-like events accelerate and decelerate along strike, driven by residual prestress from previous events, with the average rupture velocity evolving accordingly (Figure 4c).

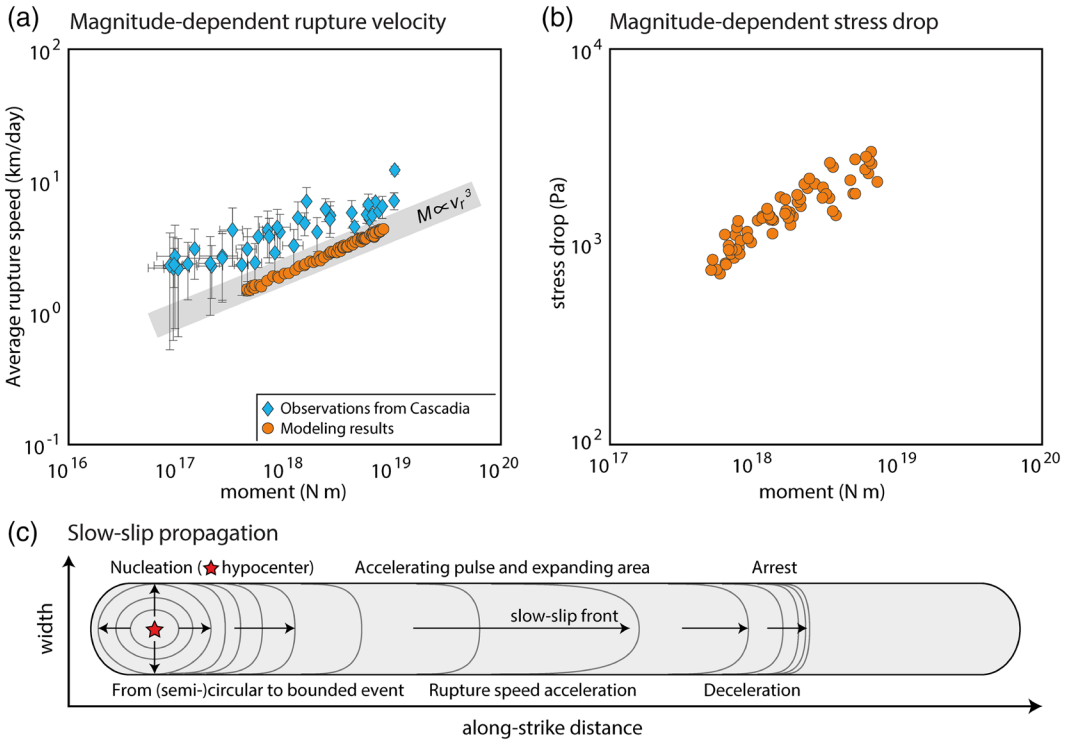

Figure 4. Magnitude-dependent rupture velocity and magnitude-dependent stress drop. (a) Average rupture velocity increases with event moment for both simulated SSEs (orange dots) and the ones observed at the Cascadia subduction zone (blue diamonds). (b) Average stress drop also increases with the event moment of the simulated SSEs. (c) Sketch summarizing the propagation of a width-bounded slow-slip event: nucleation, downdip saturation, and along-strike acceleration/deceleration of the rupture front.

4. Discussion and Conclusion

Our results show that a simple model based on standard rate-and-state friction with a single homogeneous VW patch surrounded by a VS region and loaded with dip-slip motion can produce a large population of small and large SSEs. We emphasize that, even though the SSEs follow the well-known cubic moment-duration scaling, $M \propto T^3$, they do not follow the traditional, constant-stress-drop and constant-rupture-speed circular crack model, since the stress drop and rupture speed both increase with the SSE moment. However, both observed and simulated SSEs do obey $M \propto A^{3/2}$ (because $A = L \cdot W \propto T^2$), just as for the circular crack model. Hence, stress drops computed based on the traditional model, that is, by using $\Delta\tau_{trad} = C \cdot M/A^{3/2}$ (where "*trad*" stands for traditional, C is a constant, $C = 2.44$) (Noda et al., 2013), would be automatically inferred to be magnitude-invariant for the SSEs. Of course, this pseudo "magnitude invariance" of SSE stress drops would arise from interpreting their scaling relationship $M \propto T^3$ by the (incorrect for them) circular crack model, which happens to have the same scaling. This consideration highlights the importance of not only determining the moment-duration scaling but also the appropriate explanation for it.

Note that the remarkable scaling properties of SSEs emerge even in models with standard rate-and-state friction (Figure S4). Adding dilatancy does not change the scaling but enables the model to better match observations from Cascadia, slowing down rupture speed and shifting the results toward relatively longer event durations, thus enabling a wide time spectrum ranging from a few days to several weeks and months. This stabilization occurs because, when a slip-slow event accelerates due to frictional velocity weakening, dilatancy reduces pore fluid pressure quenching the instability (Segall et al., 2010). Note also that the Gutenberg-Richter distribution of event sizes emerges naturally from our model without imposing any complexity in the spatial variation of frictional properties, due to small yet significant heterogeneous pre-stresses (Figure 2b).

In summary, our model explains the earthquake-like cubic moment-duration scaling of deep SSEs observed in Cascadia (Michel et al., 2019), Nankai (Takagi et al., 2019), and Mexico (Frank & Brodsky, 2019).

More observational and modeling studies are needed to understand whether the scaling properties we find are universal for SSEs or whether some SSEs, for example, shallow ones, can behave differently. Our results suggest that regular earthquakes and deep SSEs are both the result of frictional stick-slip motion. The pulse-like propagation, along-strike segmentation, and frequency-magnitude distribution of our simulated SSEs are remarkably similar to those observed on the Cascadia subduction zone (Michel et al., 2018). However, in contrast to the traditional assumptions, the cubic moment-duration scaling of SSEs arises not because the average rupture velocity and the stress drop of SSEs are magnitude-invariant, but rather because they increase with the increasing SSE magnitude in a particular fashion. These results not only illuminate the dynamics of SSEs but also demonstrate that the same scaling can arise for different underlying reasons. The traditional circular crack model with magnitude-invariant rupture velocities and stress drops, which is the standard explanation for the cubic moment-duration scaling, clearly does not apply to SSEs. This finding raises the question whether this traditional model and its assumptions hold even for regular earthquakes. Future advances in understanding the dynamics of fault slip will come from combining the existing and rapidly increasing streams of seismic, geodetic, and geologic data with numerical modeling informed by laboratory experiments.

Data Availability Statement

Data related to this paper can be downloaded from the following link (https://doi.org/10.22002/D1.1348).

Acknowledgments
L. D. Z. was supported by the Swiss National Science Foundation (SNSF) `P2EZP2_184307` Early Postdoc.Mobility fellowship and the Cecil and Sally Drinkward fellowship at Caltech. We thank V. Lambert, H. Kanamori, A. Gualandi, S. Michel, and Z. Ross for constructive comments and discussions. We thank the Editor and two anonymous reviewers for providing insightful comments that helped to improve the quality of this paper.

References

Bürgmann, R. (2018). The geophysics, geology and mechanics of slow fault slip. *Earth and Planetary Science Letters*, *495*, 112–134.
Bartlow, N. M. (2020). A long-term view of episodic tremor and slip in Cascadia. *Geophysical Research Letters*, *47*, e2019GL085303. https://doi.org/10.1029/2019GL085303
Dieterich, J. (2007). Applications of rate-and state-dependent friction to models of fault-slip and earthquake occurrence. *Treatise on Geophysics*, *4*, 107–129.
Dragert, H., Wang, K., & James, T. S. (2001). A silent slip event on the deeper Cascadia subduction interface. *Science*, *292*(5521), 1525–1528.
Frank, W. B., & Brodsky, E. E. (2019). Daily measurement of slow slip from low-frequency earthquakes is consistent with ordinary earthquake scaling. *Science Advances*, *5*(10), eaaw9386.
Gao, X., & Wang, K. (2017). Rheological separation of the megathrust seismogenic zone and episodic tremor and slip. *Nature*, *543*(7645), 416.
Gomberg, J., Wech, A., Creager, K., Obara, K., & Agnew, D. (2016). Reconsidering earthquake scaling. *Geophysical Research Letters*, *43*, 6243–6251. https://doi.org/10.1002/2016GL069967
Heimisson, E. R., Dunham, E. M., & Almquist, M. (2019). Poroelastic effects destabilize mildly rate-strengthening friction to generate stable slow slip pulses. *Journal of the Mechanics and Physics of Solids*, *130*, 262–279.
Ide, S., Beroza, G. C., Shelly, D. R., & Uchide, T. (2007). A scaling law for slow earthquakes. *Nature*, *447*(7140), 76.
Kanamori, H., & Anderson, D. L. (1975). Theoretical basis of some empirical relations in seismology. *Bulletin of the seismological society of America*, *65*(5), 1073–1095.
Kostrov, B. (1964). Selfsimilar problems of propagation of shear cracks. *Journal of Applied Mathematics and Mechanics*, *28*(5), 1077–1087.
Lapusta, N., & Liu, Y. (2009). Three-dimensional boundary integral modeling of spontaneous earthquake sequences and aseismic slip. *Journal of Geophysical Research*, *114*, B0930. https://doi.org/10.1029/2008JB005934
Leeman, J., Saffer, D., Scuderi, M., & Marone, C. (2016). Laboratory observations of slow earthquakes and the spectrum of tectonic fault slip modes. *Nature communications*, *7*, 11104.
Li, D., & Liu, Y. (2016). Spatiotemporal evolution of slow slip events in a nonplanar fault model for northern Cascadia subduction zone. *Journal of Geophysical Research: Solid Earth*, *121*, 6828–6845. https://doi.org/10.1002/2016JB012857
Liu, Y., & Rice, J. R. (2005). Aseismic slip transients emerge spontaneously in three-dimensional rate and state modeling of subduction earthquake sequences. *Journal of Geophysical Research*, *110*, B08307. https://doi.org/10.1029/2004JB003424
Madariaga, R. (1976). Dynamics of an expanding circular fault. *Bulletin of the Seismological Society of America*, *66*(3), 639–666.
Marone, C., Raleigh, C. B., & Scholz, C. (1990). Frictional behavior and constitutive modeling of simulated fault gouge. *Journal of Geophysical Research*, *95*(B5), 7007–7025.
Michel, S., Gualandi, A., & Avouac, J.-P. (2018). Interseismic coupling and slow slip events on the Cascadia megathrust. *Pure and Applied Geophysics*, *176*, 3867–3891.
Michel, S., Gualandi, A., & Avouac, J.-P. (2019). Similar scaling laws for earthquakes and Cascadia slow-slip events. *Nature*, *574*(7779), 522–526.
Noda, H., & Lapusta, N. (2010). Three-dimensional earthquake sequence simulations with evolving temperature and pore pressure due to shear heating: Effect of heterogeneous hydraulic diffusivity. *Journal of Geophysical Research*, *115*, B12314. https://doi.org/10.1029/2010JB007780
Noda, H., Lapusta, N., & Kanamori, H. (2013). Comparison of average stress drop measures for ruptures with heterogeneous stress change and implications for earthquake physics. *Geophysical Journal International*, *193*(3), 1691–1712.
Obara, K., Hirose, H., Yamamizu, F., & Kasahara, K. (2004). Episodic slow slip events accompanied by non-volcanic tremors in southwest Japan subduction zone. *Geophysical Research Letters*, *31*, L23602. https://doi.org/10.1029/2004GL020848
Ozawa, S. W., Hatano, T., & Kame, N. (2019). Longer migration and spontaneous decay of aseismic slip pulse caused by fault roughness. *Geophysical Research Letters*, *46*, 636–643. https://doi.org/10.1029/2018GL081465
Ozawa, S., Murakami, M., Kaidzu, M., Tada, T., Sagiya, T., Hatanaka, Y., et al. (2002). Detection and monitoring of ongoing aseismic slip in the Tokai region, central Japan. *Science*, *298*(5595), 1009–1012.

Rogers, G., & Dragert, H. (2003). Episodic tremor and slip on the Cascadia subduction zone: The chatter of silent slip. *Science*, *300*(5627), 1942–1943.

Romanet, P., Bhat, H. S., Jolivet, R., & Madariaga, R. (2018). Fast and slow slip events emerge due to fault geometrical complexity. *Geophysical Research Letters*, *45*, 4809–4819. https://doi.org/10.1029/2018GL077579

Romanowicz, B., & Rundle, J. B. (1993). On scaling relations for large earthquakes. *Bulletin of the Seismological Society of America*, *83*(4), 1294–1297.

Schwartz, S. Y., & Rokosky, J. M. (2007). Slow slip events and seismic tremor at circum-pacific subduction zones. *Reviews of Geophysics*, *45*, RG3004. https://doi.org/10.1029/2006RG000208

Segall, P., & Rice, J. R. (1995). Dilatancy, compaction, and slip instability of a fluid-infiltrated fault. *Journal of Geophysical Research*, *100*(B11), 22,155–22,171.

Segall, P., Rubin, A. M., Bradley, A. M., & Rice, J. R. (2010). Dilatant strengthening as a mechanism for slow slip events. *Journal of Geophysical Research*, *115*, B12305. https://doi.org/10.1029/2010JB007449

Shibazaki, B., & Shimamoto, T. (2007). Modelling of short-interval silent slip events in deeper subduction interfaces considering the frictional properties at the unstable—stable transition regime. *Geophysical Journal International*, *171*, 191–205. https://doi.org/10.1111/j.1365-246X.2007.03434.x

Takagi, R., Uchida, N., & Obara, K. (2019). Along-strike variation and migration of long-term slow slip events in the western Nankai subduction zone, Japan. *Journal of Geophysical Research: Solid Earth*, *124*, 3853–3880. https://doi.org/10.1029/2018JB016738

Tong, X., & Lavier, L. L. (2018). Simulation of slip transients and earthquakes in finite thickness shear zones with a plastic formulation. *Nature communications*, *9*(1), 1–8.

Wech, A. G., Creager, K. C., Houston, H., & Vidale, J. E. (2010). An earthquake-like magnitude-frequency distribution of slow slip in northern Cascadia. *Geophysical Research Letters*, *37*, L22310. https://doi.org/10.1029/2010GL044881